Numerical investigation of thermo-hydraulic performance in rib roughened fin under forced convection

Ayushman Srivastav, Kuldeep Rawat

ABSTRACT

In this paper numerical investigation of Thermo-Hydraulic performance from a rib roughened fin subjected to forced convection. Numerical data pertaining to heat transfer and friction from a rib roughened fin are generated by carrying out numerical simulations under the varied fluid flow conditions. Using a validated numerical model, the data pertaining to fluid flow and temperature distribution for different rib pitch to rib height ratio (P/e) are obtained by varying the Reynolds Number from 500 to 5000. The thermal and hydraulic performances of rib roughened fin are discussed with the help of Nusselt Number and friction factor plots. The results obtained from the rib roughened fin geometry are compared with that of a plain fin to determine the effectiveness of test fin in extracting heat from its base under similar operating conditions. The rib roughened fin having P/e of 6 which bring out maximum enhancement in the heat transfer and friction.

Index Terms: Rib Roughened fin; Nusselt number; Friction factor; Reynolds number.

1. INTRODUCTION

Fins are used in a variety of engineering applications to enhance the convective heat transfer rate by achieving a large total heat transfer surface area without the use of an excessive amount of primary surface area. A fin is made of thermally conductive materials that extracts heat from its base and pass it on to the surrounding fluid through the large surface area. The design of cooling fins is encountered in many situations where the rate of heat transfer from a heat exchange surface plays a vital role in finalizing the shape, size and material for the systems. Several researches have been carried out to explore the effect of the system and flow parameters on the thermal performance of the engineering systems. The experimental and numerical approaches were adopted to study the heat transfer and friction characteristics of fin arrays so that the optimal geometric parameters can be selected under a specified operating conditions. Due to simple shape and ease in manufacturing, rectangular plate fins and pin fins are preferred in the majority of heat transfer applications. J. C. Han et al. [1] performed experiments on the rib-roughened surface to determine the effects of rib shape, angle of attack and pitch to rib height ratio on friction factor and heat-transfer results. They developed a general correlation for friction factor and heat transfer as function of rib shape, spacing and angle of attack and also reported that ribs at a 45^o angle of attack have superior heat transfer performance at a given pumping power. Rongguang Jia et al. [2] carried out a numerical investigation to determine the velocity and heat transfer characteristics of multiple impinging slot jets in rib-roughened channels. He considered different size and arrangement of jets and ribs and reported that the ribs enhance the heat transfer, if they are well arranged. Both the position and size of the ribs are of importance for heat transfer in rib-roughened channel. Larger recirculation zones induced by the jets near the roughened wall result in higher heat transfer coefficients. G. Iaccarino et al. [3] investigated the effect of thermal boundary conditions on numerical heat transfer predictions in rib-roughened passages. They obtained results using constant heat flux. Their experimental measurements and data correlations showed that the predicted heat transfer is very sensitive to the type of boundary conditions used in the numerical model. It was illustrated that some of the discrepancies observed between experimental and numerical data can be eliminated if conduction heat transfer in the rib is taken into account. In the experimental study, P. M. Ligrani et al. [4] presented the spatially resolved Nusselt number, spatially averaged Nusselt number, and friction factor for a stationary channel roughened with the angled rib turbulators inclined at 45^o. Their results showed that the spatially resolved local Nusselt number reached to the maximum value at the top face of the rib turbulators, while the regions of flow separation and shear layer reattachment have pronounced influence on local surface heat transfer behavior. Xiufang GAO et al. [5] has shown

- *Ayushman Srivastav is Assistant professor at Department of mechanical Shivalik College of Engineering Dehradun, India, PH-+91-9410593973. E-mail: Ayushman.srivastav@gmail.com*

that the flow behavior in rib-roughened duct is influenced by the inclination of ribs. Their study showed that the rib orientations not only affect the secondary flow style and its strength, but also alter the mean flow velocity distribution along the span wise direction and the secondary flow were found to be strongest for the one created by the ribs at 45o. M.K.Gupta and S.C. Kaushik. [6] Conducted a comparative study of various types of artificial roughness geometries applied on the absorber plate of solar air heater duct to explore the heat transfer and friction characteristics and found that for the higher range of Reynolds number circular ribs and V shaped ribs give appreciable improvement in the exergy efficiency for the higher values of Reynolds number; chamfered rib–groove geometry gives higher exergy efficiency for relatively low values of Reynolds number. Bilen et al. [7] studied the effect of the geometric position of wall-mounted rectangular blocks on the heat transfer from the surface by carrying out experimental work. They reported that the most important parameter affecting the heat transfer is Reynolds number. It has been observed that heat transfer can be successfully improved by increasing the Reynolds number and the second most effective parameter for increasing the heat transfer is the turning angle of the blocks Apurba Layek [8] worked for optimization of roughness parameters of solar air heater based on effective efficiency criterion. He reported that solar air heater having absorber plate having chamfered rib – groove roughness shows higher thermal gain compared to smooth collectors with nearly same pressure drop penalty. They also have a better effective efficiency as compared to conventional smooth air heaters. Shaeri et al. [9] numerically determined the heat transfer and frictional losses from an array of solid and perforated fins mounted on a flat plate. Perforated fins have windows with square cross section and arranged in different numbers. Results showed that perforated fins have higher total heat transfer rates with considerable weight reduction in comparison to the solid fins. It was reported that the perforated fins have relatively lesser drag and the drag ratio decreases by increasing the Reynolds number. With the increase of Reynolds number, the percentage of heat transfer enhancement with respect to solid fin depreciates in most of the cases for perforated fins.. Iftikarahamad H. Patel and Sachin L. Borse [10] worked on the experimental investigation of the forced convection heat transfer over the dimpled surface. In a similar study, Do Seo Park [11] has explored the dimpled heat sink subjected to the laminar airflow. This was accomplished by performing an experimental and numerical investigation using circular (spherical) dimples, and oval (elliptical) dimples. He showed that with the increase of Reynolds number thermal performances of circular and oval dimpled fin increases. The thermal performance of fins having oval dimples was found to be higher than that of the circular dimples. Anil Singh Yadav and J. L. Bhagoria [12] worked on a CFD-based model of turbulent flow through a solar air heater roughened with square-sectioned transverse rib roughness. They reported that the average heat transfer, average flow friction, and thermo hydraulic performance parameter are strongly dependent on the relative roughness height.

The object of present work is to determine the heat transfer and friction characteristics of flat plate fin with the repeated ribs on its two broad surfaces under forced convection using the standard numerical techniques. In order to assess the heat transfer performance of the test fin, effectiveness of ribbed fin is determined with respect to a plain fin for the same boundary conditions. For this, the data pertaining to heat transfer and friction at various fluid flow rates have been generated by solving the governing equations under the specified boundary conditions for different ribbed fin geometry. The enhancement in heat transfer and friction with regard to different ribbed fin parameters are compared with that of a plain fin under varied fluid flow Reynolds number.

2. PROBLEM DESCRIPTION AND COMPUTATIONAL DOMAIN

The computational domain chosen for a test fin as guideline suggested by Franke [13]. Referring to the Fig.1, a test fin is attached to the base plate which is considered to be an isothermal surface. The air flow is considered to be steady with the temperature dependant thermo physical properties. The air velocities are varied in a range such that the flow pattern can be transformed from laminar to turbulent nature having forced convection heat transfer between the ribbed fin and surrounding air. The aluminium is selected for fin material due to the higher conductivity and lower weight. The test fin length (L) is taken as 48 mm, whereas the height (hf) and thickness (D) of fin are considered as 12 mm and 4 mm respectively.

The computational domain consists of an entrance section, an exit section and the upper free stream surface as planes ‘abcd’, ‘ijkl’ and ‘bckj’ respectively. The lengths of the entry and exit regions are of 5hf and 10hf on the upstream and downstream side of the fin, respectively. The domain extends 6hf in Y direction and 4hf in Z direction excluding the fin. At the inlet section ‘abcd’, uniform flow conditions are considered by defining the velocity components at the inlet as: $u_{in} = u_{\infty}$; $v_{in} = w_{in} = 0$ and $T_{in} = T_{\infty}$. Free stream conditions are applied to plane ‘bckj’. The exit plane ‘ijkl’ is sufficiently far from the plate ‘efgh’, therefore negligible temperature and

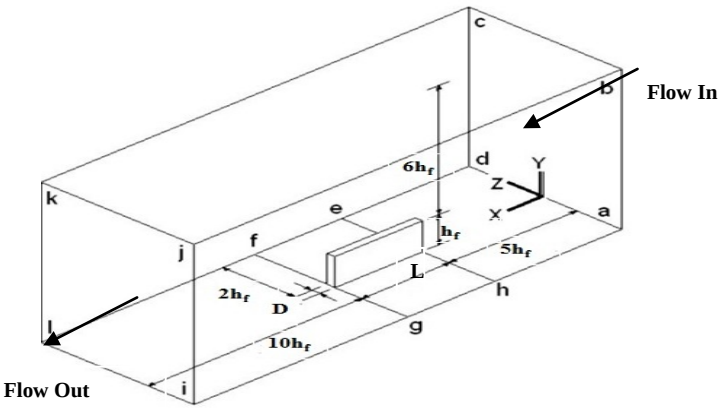

Fig.1: Computational domain.

pressure gradients are assumed along X direction. All the remaining planes are assumed as solid adiabatic walls with no slip conditions at the surfaces. The temperature of fin base plane 'efgh' (T_b) is assumed to be constant as 70°C whereas the free stream temperature of fluid (T_∞) is taken as 25° C.

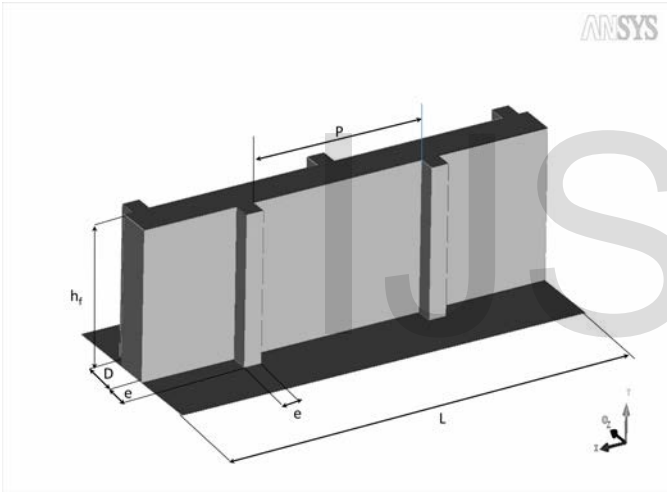

Fig.2: Ribbed fin geometry.

Leung and Probert [14] have reported that thermal radiation rate is found to be less than 8% of total heat transfer rate from the finned surfaces for polished aluminium fins if the temperature difference is kept less than 77.5° C. In agreement to the above observation, the effect of radiation heat transfer is neglected in the present work since the maximum temperature difference in the present study is 45° C. Square ribs are created on both the sides of the solid fin, all along its length at the specified pitch. The geometrical parameters of ribbed fin are shown in Fig.2. The ribs of height (e) are arranged in the direction normal to the flow and are separated by pitch (P). The relative rib pitch (P/e) is defined as the ratio of rib pitch to rib height. The results of grid independency study for a plain fin are shown in Table 1. It can be noticed that the considerable changes in the values of Nusselt number and friction factor are observed due to the refinement in the grid configuration. The change in the Nusselt number and friction factor values were found to be less than 0.83% and 1.10% beyond the grid size of 164×35×11 for the fin and 9×223×130 for the whole domain.

Table 1: Grid independency test for a plain fin (Re = 5000).

Grids in whole domain (X×Y×Z)	Grids in plain fin (X×Y×Z)	Nusselt Number (Nu)	Friction factor (f)
228×84×52	48×12×4	14.48	0.00351
353×94×65	54×14×5	16.23	0.00491
425×112×78	64×17×6	17.69	0.00544
527×155×86	110×21×8	18.77	0.00563
632×186×103	120×25×9	20.28	0.00598
679×223×130	164×35×11	20.45	0.00606

3. NUMERICAL METHOD

3.1 RNG k-ε turbulent model

The RNG k-epsilon (k- ε) model is used to model the turbulent flow in the present work to compliment the conditions that the flow is incompressible with constant thermal conductivity, no heat dissipation, no compression work and no heat generation. The turbulence is assumed to be homogeneous and isotropic and therefore, the turbulence kinetic energy k, and its rate of dissipation ε, are given by following two equations

$$\rho(u\frac{\partial k}{\partial x}+v\frac{\partial k}{\partial y}+w\frac{\partial k}{\partial z})=[(\mu+\frac{\mu_t}{\sigma_k})(\frac{\partial^2 k}{\partial x^2}+\frac{\partial^2 k}{\partial y^2}+\frac{\partial^2 k}{\partial z^2})]+G_k-\rho\varepsilon \quad (1)$$

And turbulent energy dissipation rate equation is

$$\rho(u\frac{\partial \varepsilon}{\partial x}+v\frac{\partial \varepsilon}{\partial y}+w\frac{\partial \varepsilon}{\partial z})=[(\mu+\frac{\mu_t}{\sigma_\varepsilon})(\frac{\partial^2 \varepsilon}{\partial x^2}+\frac{\partial^2 \varepsilon}{\partial y^2}+\frac{\partial^2 \varepsilon}{\partial z^2})]+C_{1\varepsilon}\frac{\varepsilon}{k}G_k-C_{2\varepsilon}\rho\frac{\varepsilon^2}{k} \quad (2)$$

Where Gk represents the generation of turbulent kinetic energy due to mean velocity gradients, and can be calculated using Boussinesq hypothesis as Gk = μt S2, where S is the modulus of the mean rate-of-strain tensor, defined as $S \equiv \sqrt{(2S_{ij}\,S_{ij})}$ and S_{ij} can be defined as

$$S_{ij} = \frac{1}{2}\left(\frac{\partial \overline{u_i}}{\partial x_j} + \frac{\partial \overline{u_j}}{\partial x_i}\right) \quad (3)$$

The turbulent (or eddy) viscosity μt is computed by combining k and ε as follows:

$$\mu_t = \rho C_\mu \frac{k^2}{\varepsilon} \quad (4)$$

The model constants for the two transport equations C1Ɛ, C 2Ɛ, Cμ, σk and σƐ have the following values C1Ɛ= 1.42; C 2Ɛ=1.68; Cμ=0.085; σk=1.0; σƐ=1.3

3.2 Solution method

FLUENT 14.0 is used to solve the incompressible RANS equations using a second order upwind scheme chosen for energy and momentum equations and the SIMPLE pressure–velocity coupling technique.

4. VALIDATION

To validate the present numerical scheme the results of computational model are compared with the experimental results presented by Nakamura et al. [15]. Nakamura et al. [15] performed experimental studies to investigate the fluid flow and the local heat transfer around the cube mounted on the wall of the plane for the Reynolds number 4,200 – 33,000 and reported the following relation between the mean value of Nusselt number and the Reynolds number: (5)

$$Nu_m = 0.137\ Re^{0.68}$$

By using the equation $Nu_m = 0.137\ Re^{0.68}$, mean Nusselt number was calculated for cube mounted on the wall with respect to different Reynolds number. In order to compare the heat transfer data obtained by the present numerical scheme with the data obtained from the correlations suggested by Nakamura et al. [15], the values of Nusselt number are plotted as function of Reynolds number. The comparative plot in Fig.3 shows good agreement between the present numerical data and corresponding data found from correlations. The average absolute deviation of the present numerical data from the correlation data is found to be 3.7% which falls within the acceptable limits. The minute deviation might be due to differences of inlet boundary layer, differences in turbulent intensities, numerical discritization and uncertainties in the meshing.

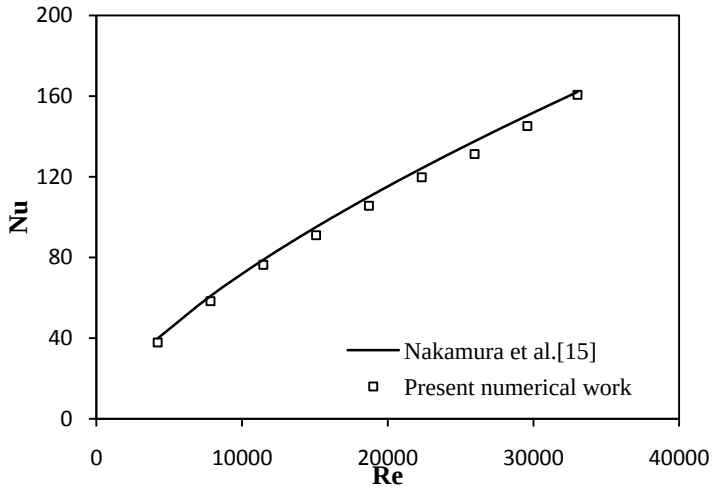

Fig.3: Comparison of numerically predicted Nusselt number and the experimental Nusselt number [15].

5. Results and discussion

The validated numerical scheme is used to generate the data pertaining to heat transfer and friction from a ribbed fin under forced convection. The heat transfer and friction characteristics of ribbed fin are discussed with the help of fin heat transfer, Nusselt and friction factor plots as function of system and operating parameters. The heat transfer performance of ribbed fin is also discussed with the help of Nusselt number enhancement ratio (Nur/Nup) and Thermo hydraulic performance (η) for different fin configurations while flow Reynolds number is varied from 500 to 5000. It is evident that, the heat transfer rate from a fin under forced convection is a strong function of the nature of fluid flow in the boundary layer. It has been observed that the fin dissipates heat energy at a considerably higher rate, when the fluid flow rate is increased.

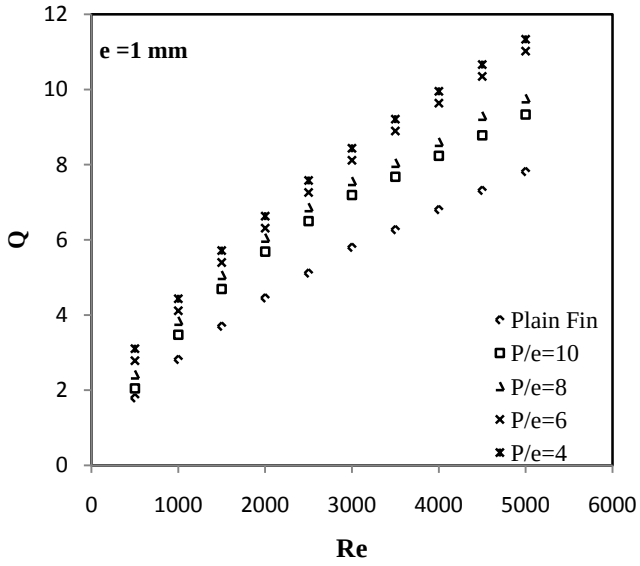

Fig.4: Variation of fin heat transfer rate with Reynolds number for different relative rib pitch (P /e) at e = 1mm.

It is believed that the application of turbulators in the form of ribs or any other form of surface irregularity such as grooves or perforations promotes disturbance near the wall and thereby yields higher heat transfer rates at the cost of additional pressure drop. Fig.4. shows the fin heat transfer rate as function of flow Reynolds number for different values of rib pitch to rib height ratio corresponding to rib height of 1 mm. It can be observed that the values of heat transfer rate are found to increase with increasing the value of Reynolds number in all cases. Plot reveals that the ribbed fin yields considerable higher heat transfer than that of a plain fin. The vortices induced around the square ribs and the overall increase in surface area of the fin is responsible for the enhanced heat transfer rates. The heat transfer rate increases as the relative rib pitch (P/e) decreases.

The effect of relative rib pitch (P/e) on the heat transfer rate from ribbed fin surface is shown in Fig.5. The maximum heat transfer corresponds to the relative rib pitch (P/e) of 4 that produces notable increase in heat transfer in comparison to the plain fin at all values of Reynolds number. Fig.6 shows the variation of Nusselt number as the Reynolds number is varied between 500-5,000 for different values of relative rib pitch (P/e) along with the plain fin for a comparative study.

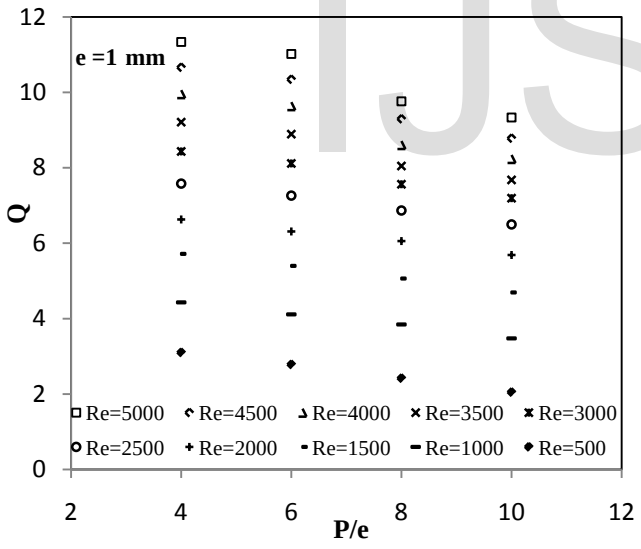

Fig.5: Variation of fin heat transfer rate with Relative Rib Pitch (P /e) for different Reynolds number at e = 1mm.

Considerable jump in the Nusselt number values can be seen in all the cases as compared to the plain fin. To understand the variation of Nusselt Number, with the change in relative rib pitch (P/e), Fig.7 is plotted. It can be seen that at all the values of Reynolds number, the Nusselt number increases with the increase in the value of relative rib pitch up to 6, beyond which, it decreases with further increase in relative rib pitch.

It is believed that the repeated ribs over the surface cause flow separations and reattachments which leads to the substantial change in the local heat transfer rates. Previous studies show that the maximum heat transfer occurs at the vicinity of reattachment point where boundary layer begins to grow before the succeeding rib is reached. This may have resulted in the observation of the maximum value of the Nusselt number at a certain value of relative rib pitch.

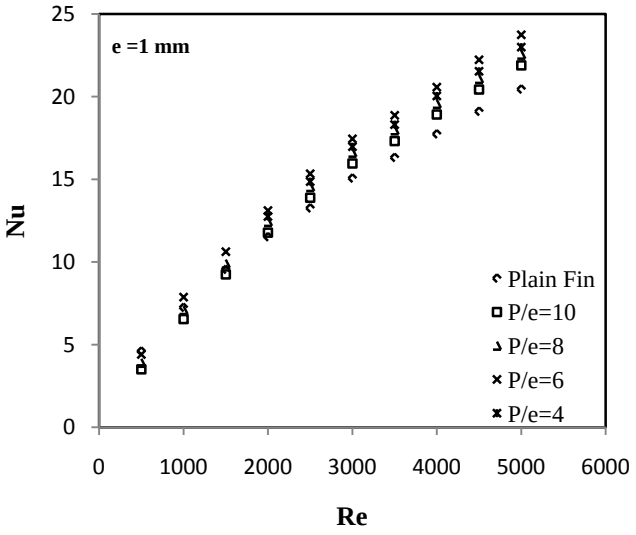

Fig.6: Variation of fin Nusselt number with Reynolds number for different relative rib pitch (P /e) at e = 1 mm.

With a view to understand the heat transfer characteristics of a ribbed fin, temperature contours for relative rib pitch of 6 are shown in Figs.8 and 9. It can be observed that the temperature of ribbed fin surface towards the leading end is on lower side. It is due to the fact that the cold air stream experiences higher temperature gradient while approaching the leading edge of fin and, thereby, observes higher heat transfer rates. Careful study of temperature contours unfolds that the lowest values of temperature are found somewhere in between the two ribs apart from the leading edge of the fin. The higher heat removal rate in between two ribs can be attributed to the reattachment of flow to the fin surface; moreover, there is a local contribution to the heat removal by the vortices originating from the rib roughness. Fig.10 shows the effect of flow Reynolds number on friction factor with regard to different relative rib pitch (P/e). The plot shows that the friction factor decreases as the flow Reynolds number is increased for all fin geometries because of thinning of viscous sub layer as Reynolds number approaches to higher values.

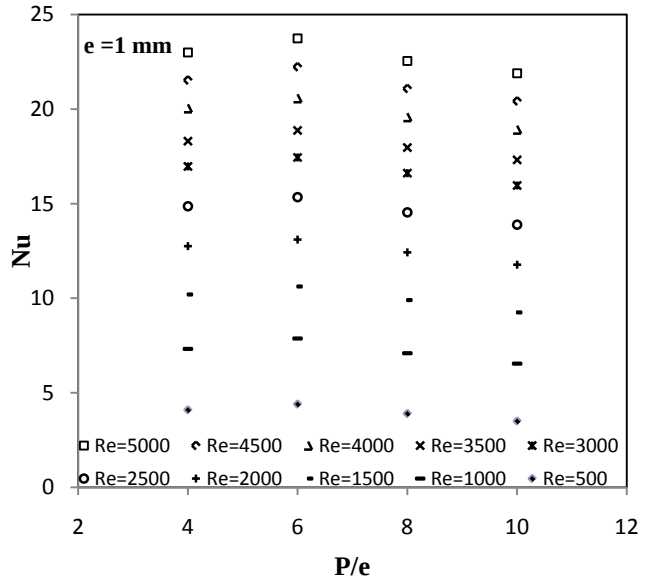

Fig.7: Variation of fin Nusselt Number with Relative Rib Pitch (P /e) for different Reynolds number at e = 1 mm.

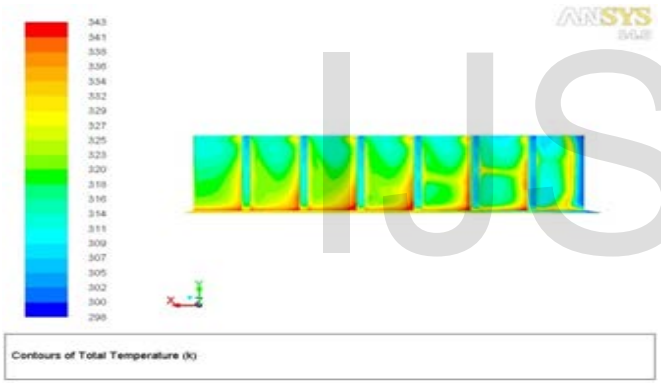

Fig.8: Front view of a ribbed fin showing temperature contours. (e=1mm; P /e = 6; Re=5000)

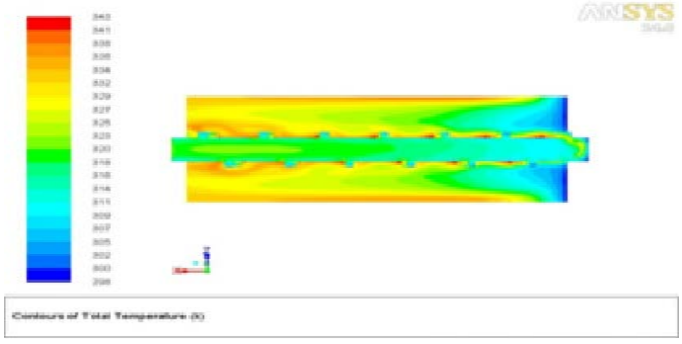

Fig.9: Top view of a ribbed fin showing temperature contours. (e = 1 mm; P /e = 6; Re=5000)

It can be seen that there is a substantial enhancement caused as a result of providing rib roughness in the form of square-rib oriented in a transverse direction. Notable increase in the friction factor can be observed for the ribbed fin as compared to a plain fin subjected to similar operating conditions.

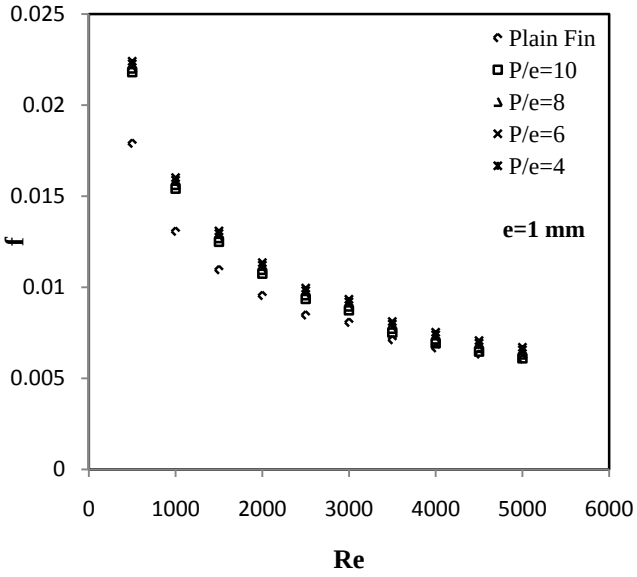

Fig.10: Variation of fin Friction factor with Reynolds number for different relative rib pitch (P /e) at e = 1 mm

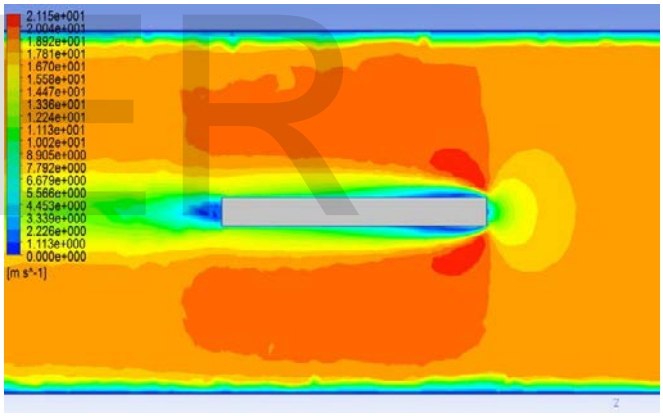

Fig.11: Velocity contour of the plain fin at Re=5000

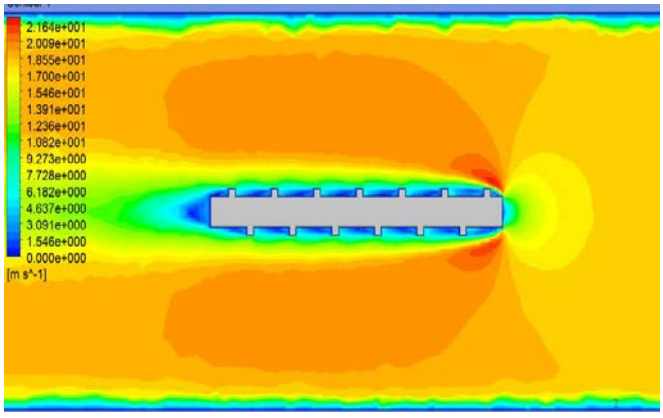

Fig.12: Velocity contour of a ribbed fin (e = 1 mm; P /e = 6; Re=5000)

Figs.11 and 12 show the comparison between the flows over the plain fin and the ribbed fin profile, there is a

stream line flow over the plain fin whereas the flow is seen to be separated at the rib which appears to be reattached with the surface in the vicinity of succeeding rib. It is seen that the separated boundary layer behind the rib results in a dead zone by forming the vortex near the rib which reduces the heat transfer through this area. Fig.13. shows the vector contour, the direction of movement of stream clearly indicating the formation of dead zone and reattach contour at the vicinity of succeeding rib.

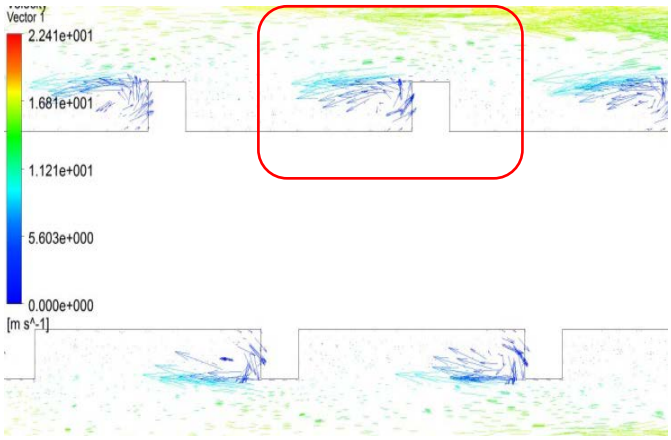

Fig.13: Velocity vector contour showing the direction of flow (e=1 mm; P/e=6; Re=5000)

Fig. 14 shows the effect of Reynolds number on the Nusselt number enhancement ratio $\left(\frac{Nu_r}{Nu_p}\right)$ for different values of relative rib pitch (P/e) corresponding to the rib height (e) of 1 mm. It can be observed that the ribbed fin having relative rib pitch (P/e) of 6 outperforms the other fin geometries. Fig.15 shows the variation of friction factor ratio $\left(\frac{f_r}{f_p}\right)$ for different values of relative rib pitch at the rib height (e) of 1 mm. Friction factor ratio is decreased with the increase in the value of Reynolds number; however, the slope of friction factor ratio curve is steepest in case of (P/e) of 10 than smaller values of (P/e). Consequently any enhancement scheme must be evaluated by the simultaneous consideration of thermal and hydraulic performance of the system. A well-known method of such evaluation was proposed by Webb and Eckert [16] in the form of thermo- hydraulic performance parameter.

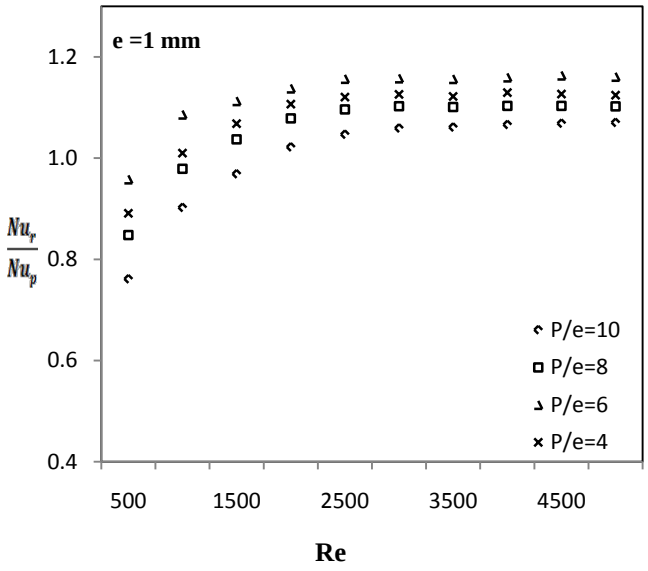

Fig.14: Variation of Nusselt number enhancement ratio with Reynolds number for ribbed fin at e =1 mm.

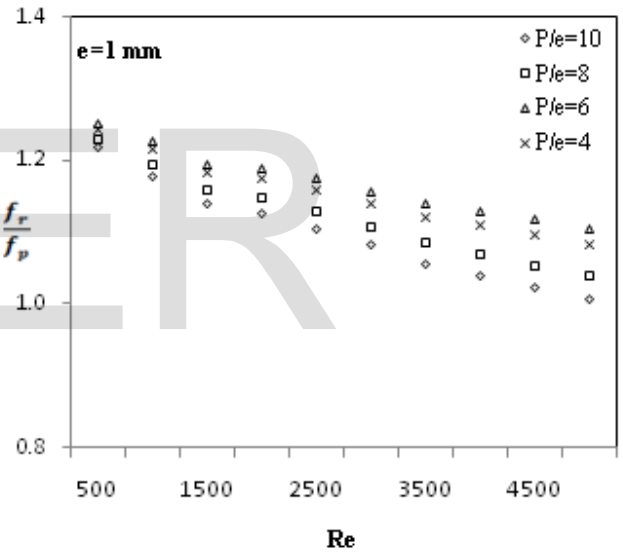

Fig.15: Variation of Friction factor ratio with Reynolds number for ribbed fin at e =1 mm.

The thermo-hydraulic performance parameter is defined as the ratio of the Nusselt number of a roughened surface to that of a smooth surface at an equal pumping power.

$$\text{Thermo-hydraulic performance parameter } (\eta) = \frac{(Nu_r/Nu)}{(f_r/f_p)^{\frac{1}{3}}} \quad (6)$$

Fig.16 shows that the thermo-hydraulic performance of rib roughened fin increases as the Reynolds number increases in cases of rib height equal to 1 mm. It is observed that the maximum value of thermo-hydraulic performance occurs at relative rib pitch (P/e) of 6 at all the values of Reynolds number.

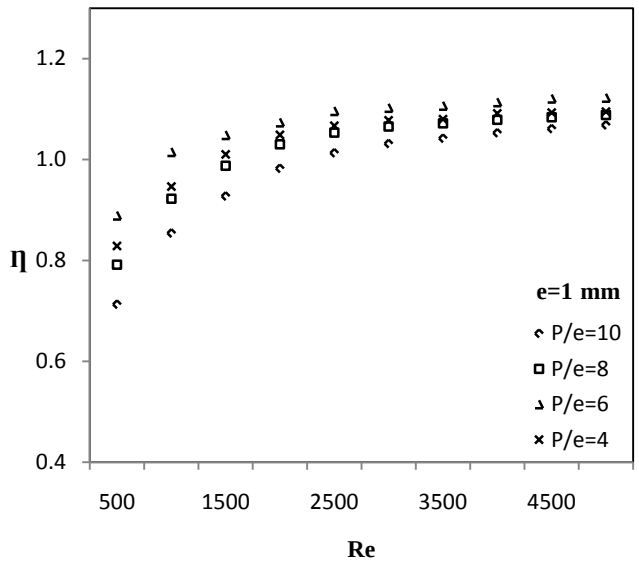

Fig.16: Thermo-hydraulic performance as function of Reynolds number for ribbed fin at e =1 mm.

6. Conclusions

The present work deals with the study of heat transfer and friction characteristics of a ribbed fin by using computational approach. On the basis of present study, following conclusions is drawn:

The ribbed fin brings out significant enhancement in heat transfer with the concurrent increase in frictional losses with respect to a plain fin. The relative rib pitch (P/e) of 6 showed nearly two folds enhancement in the heat transfer as compared to the plain fin performance.

The Nusselt number increases and friction factor decreases with an increase in the values of Reynolds number for all cases. The maximum enhancement in the Nusselt number and the friction factor corresponds to the relative rib pitch (P/e) of 6.

The thermo-hydraulic performance parameter of rib roughened fin attains its maximum value corresponding to the rib pitch of 6.

Nomenclature

Ab	Cross-section area of the base plate	T	Temperature
Af	Cross-section area of the fin	Tin = T∞	Mean plate temperature
Cp	Specific heat	Wp	Width of perforation
Cp,Al	Specific heat of aluminium	uin = u∞	Inlet velocity of air
D	Fin thickness	X,Y,Z	rectangular coordinate
Dh	Equivalent hydraulic diameter of duct	P/e	Relative rib pitch
e	Height of the rib		
f	Friction factor	Greek symbols	
h	Convective heat-transfer coefficient	α	Under-relaxation factor
hf	Fin height	Δ	Difference
hp	Height of perforation	μ	Dynamic viscosity
kAl	Thermal conductivity of aluminium	ρ	Density of air at bulk mean air temperature
k	Turbulent kinetic energy		
Pr	Prandtl number	Φ	General variable
Q	Heat transfer rate to air	∇	The vector differential operator
R	Residual		
Re	Reynolds number	ε	turbulent dissipation rate
t	Time	η	Thermo hydraulic performance

References

[1] Han J. C., Glicksmanan L.R. and Rohsenow W. M. "An investigation of heat transfer and friction for rib-roughened surfaces", Int. J. Heat & Mass Transfer, Vol. 21; pp. 1143-1156

[2] Rongguang Jia, Masoud Rokni and Bengt Sunde´n "Impingement cooling in a rib-roughened channel with cross-flow", International Journal of Numerical Methods for Heat & Fluid Flow, Vol. 11; No. 7, pp. 642-662 (2001).

[3] Iaccarino G., Ooi A. and Durbin P.A. , Behnia M. "Conjugate heat transfer predictions in two-dimensional ribbed passages", International Journal of Heat and Fluid Flow, Vol. 23; pp 340–345 (2002).

[4] Ligrani P. M. and Mahmood G. I. "Spatially Resolved Heat Transfer and Friction Factors in a Rectangular Channel With 45-Deg Angled Crossed-Rib Turbulators", ASME, Vol. 125; Issue July, pp 575-584 (2003).

[5] Xiufang Gao and Bengt Sunde´n "Effects of Inclination Angle of Ribs on the Flow Behavior in Rectangular Ducts", ASME Vol. 126; Issue July, pp 692-699 (2004).

[6] Gupta M.K. and Kaushik S.C. "Performance evaluation of solar air heater for various artificial roughness geometries based on energy, effective and exergy efficiencies", Renewable Energy, Vol.34; pp 465–476 (2009).

[7] Bilen K., Yapici S. and Celik C., "A Taguchi approach for investigation of heat transfer from a surface equipped with rectangular blocks", Energy Convers Manage, Vol.42; pp 951–961, (2001).

[8] Layek Apurba. "Optimal thermo-hydraulic performance of solar air heater having chamfered rib-groove roughness on absorber plate", IJEE, Vol. 1; Issue 4, pp 683-696 (2010).

[9] Shaeri, M.R., Yaghoubi, M., "Heat transfer analysis of lateral ribbed fin heat sinks", Applied Energy, Vol.86; pp 2019–2029, (2009).

[10] Patel I.H. and Borse Sachin.L. "Experimental investigation of heat transfer enhancement over the dimpled surface", IJEST, Vol. 4; Issue.08, August pp 3666-3672 (2012).

[11] Seo P. D. "Experimental and numerical study of laminar forced convection heat transfer for a dimpled heat sink", A Thesis Submitted to the Office of Graduate Studies of Texas A&M University (2007).

[12] Yadav Anil Singh and Bhagoria J. L. "Modeling and Simulation of turbulent flows through a solar air heater having square-sectioned transverse rib roughness on the absorber plate", The Scientific World Journal Volume, Article ID 827131 (2013)

[13] Jörg Franke, Antti Hellsten, Heinke Schlünzen, and Bertrand Carissimo "Best practice guideline for the CFD simulation of flows" COST Action 732 , (2007).

[14] Leung C.W, Probert S.D., "Heat exchanger performance: effect of orientation", Appl Energy, Vol. 55; pp 33:35, (1989).

[15] Nakamura H., Igarashi T. and Tasutsui T., "Local heat transfer around wall-mounted cube in the turbulent boundary layer" Int. J. Heat & Mass Transfer, Vol. 44; pp. 3385-3395 (2001).

[16] Webb R. L., and Eckert R.G, "Application of rough surfaces to heat exchanger design," International Journal of Heat and Mass Transfer, Vol. 15, Issue. 9, pp. 1647–1658, 1972.